

# Signal Processing and Analyzing Works of Art

Don H. Johnson<sup>a</sup>, C. Richard Johnson, Jr.<sup>b</sup>, Ella Hendriks<sup>c</sup>

<sup>a</sup>Rice University, Houston, Texas USA

<sup>b</sup>Cornell University, Ithaca, New York, USA

<sup>c</sup>van Gogh Museum, Amsterdam, The Netherlands

## ABSTRACT

In examining paintings, art historians use a wide variety of physico-chemical methods to determine, for example, the paints, the ground (canvas primer) and any underdrawing the artist used. However, the art world has been little touched by signal processing algorithms. Our work develops algorithms to examine x-ray images of paintings, not to analyze the artist's brushstrokes but to characterize the weave of the canvas that supports the painting. The physics of radiography indicates that linear processing of the x-rays is most appropriate. Our spectral analysis algorithms have an accuracy superior to human spot-measurements and have the advantage that, through "short-space" Fourier analysis, they can be readily applied to entire x-rays. We have found that variations in the manufacturing process create a unique pattern of horizontal and vertical thread density variations in the bolts of canvas produced. In addition, we measure the thread angles, providing a way to determine the presence of cusping and to infer the location of the tacks used to stretch the canvas on a frame during the priming process. We have developed weave matching software that employs a new correlation measure to find paintings that share canvas weave characteristics. Using a corpus of over 290 paintings attributed to Vincent van Gogh, we have found several weave match cliques that we believe will refine the art historical record and provide more insight into the artist's creative processes.

**Keywords:** spectral analysis, x-ray, radiograph, canvas weave, van Gogh

## 1. INTRODUCTION

To investigate the history and authenticity of paintings by the great masters, signal processing algorithms can provide new insights.<sup>1</sup> Our focus here is on x-ray images that can reveal much about what's below the visible surface.<sup>2,3</sup> Figure 1 shows an x-ray taken of a painting by Vincent van Gogh. The brushstrokes of partially x-ray-opaque paints are clearly evident, as well as the wood stretcher and the tacks that attach the canvas to the stretcher. A close examination of the x-ray reveals the thread pattern of the canvas support (Figure 1b). Although the threads are transparent to x-rays, artists typically prepared their canvases with a lead white-containing undercoat (also called a primer or ground layer) to smooth the surface. The small variations in undercoat thickness filling the valleys of the canvas weave lead to variations in x-ray opacity that can be easily seen. Thread count data—measurements of the horizontal and vertical thread densities—are commonly used as evidence for dating, linking pictures from the same canvas roll, and attribution.<sup>2-4</sup> Thread counting algorithms seek the weave density, measured in threads/cm, in both the horizontal and vertical directions and how these counts vary throughout the painting. The current standards for any measurement technique are manual measurements made with a ruler from a few selected locations in the painting and a human counting of the number of threads in horizontal and vertical directions, a tedious process to say the least. The Thread Count Automation Project seeks to develop signal processing algorithms that can detail the variations in the canvas thread density across a painting<sup>5</sup> and to search for other paintings having a canvas weave pattern that matches it.

Before bringing signal processing methods to bear on the thread counting problem, considering how a loom works reveals how to think about thread count measurements. The vertical threads mounted in a loom, known as the *warp*, are usually well aligned with a fairly uniform spacing. The horizontal threads, known as the *weft*, are passed back and forth through the warp in an interlaced fashion, with the weft compacted after each pass to strengthen the cloth. In most cases, the weft shows more variability than the warp. When cutting a piece of canvas for a painting, the artist will orient the canvas on the stretcher in whatever way seems best: the warp direction may correspond to either the vertical or horizontal threads in

---

Further author information: D.H.J.: dhj@rice.edu, +1 713 348 4956, C.R.J.: johnson@ece.cornell.edu, +1 607 255 0429, E.H.: hendriks@vangoghmuseum.nl. Correspondence should be addressed to D.H.J.

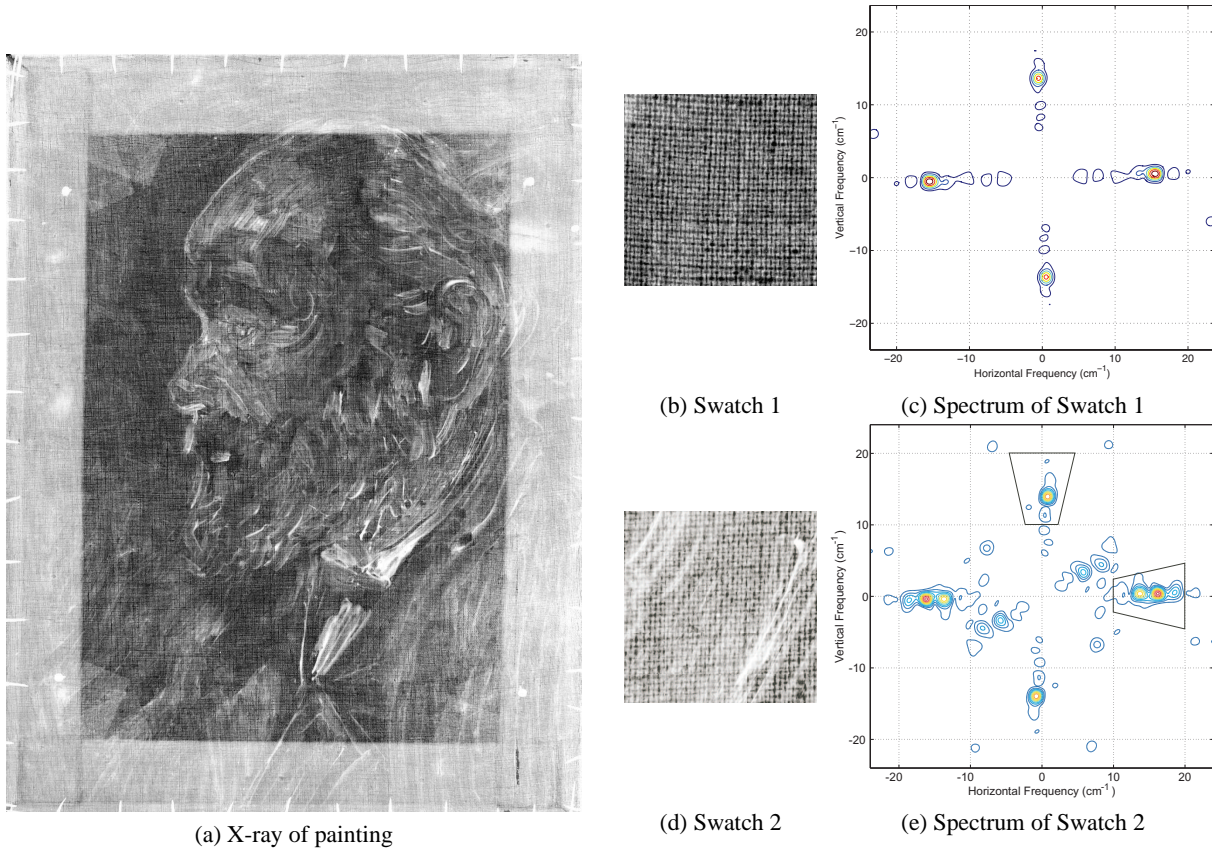


Figure 1: Panel (a) depicts the x-ray image of van Gogh’s *Portrait of an Old Man with a Beard* (F205 in the catalog of de la Faille<sup>6</sup>). The painting, the wood stretcher (the lighter border) and canvas-mounting nails can be clearly seen. Magnifying the x-ray reveals the canvas weave as well. Panels (b) and (d) show 1" × 1" swatches taken from the x-ray of F205. Panel (b) is taken from the area in front of the face; panel (d) is taken from the area below the ear. Panels (c) and (e) show detailed spectra computed from a smaller square (1 cm × 1 cm) located in the upper left corner of each swatch. The wedges indicate areas where weave-related spectral peaks are found. Image sampled at 600 dpi and provided by the Van Gogh Museum.

the painting. The width (standard deviation) of the thread count distribution provides a strong clue as to how the canvas was cut from the roll: one would expect the thread count having the narrower distribution to be the warp direction [3, p. 100]. Thread counts, along with other forensic and historical data, allow the art historian to pose strong hypotheses about how the canvas roll was used for paintings contemporary with each other. For example, in his Dutch and late French periods, Vincent van Gogh ordered canvas in rolls and, for small to moderate sized paintings, he would cut a rectangular section and mount it on a stretching frame with tacks. The hypothesis is that if two canvas sections share a horizontal or vertical position on the canvas roll, the thread density variations along that axis should agree. Consequently, works associated with the same canvas roll can be presumed to have been painted at about the same time. Since van Gogh worked alone during much of his career, weave-matched paintings could be assumed to be painted by him.

We have taken a frequency-domain approach to performing automatic thread counting. The justification for this approach begins by considering the physics of radiography. The greater the radiographic-absorbing paint thickness along the beam, the greater the opacity, meaning that x-ray image intensity variations correspond to paint composition and thickness. Letting  $i(x,y)$  denote x-ray intensity at a point on the image and  $z$  the direction of x-ray propagation, and  $o(x,y,z)$  the opacity at the x-ray frequency, basic physics of scattering relates intensity and opacity by

$$i(x,y) = \exp \left\{ - \int o(x,y,z) dz \right\} . \quad (1)$$

The canvas weave is made visible by the thicker ground (primer) layer of lead-white paint in the grooves between canvas

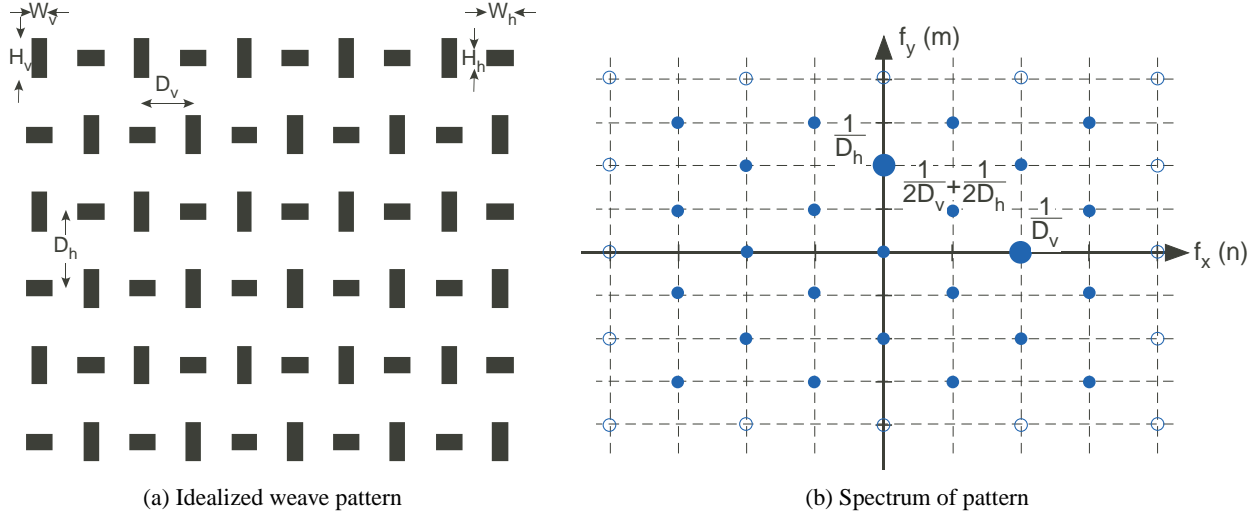


Figure 2: Panel (a) depicts an ideal weave expressed by equation (2). Here,  $D_h = 1.5D_v$ ,  $W_h = D_v/2$ ,  $H_h = D_h/5$ ,  $W_v = 2D_v/7$ ,  $H_v = D_h/2$ . The frequencies at which the canvas weave spectrum of the ideal pattern of panel (a) can be non-zero are shown in panel (b). Note that  $\frac{1}{D_v}$  on the  $x$ -frequency corresponds to the vertical thread count and  $\frac{1}{D_h}$  on the  $y$ -frequency axis to the horizontal thread count. The unfilled circles correspond to frequencies that are identically zero because of the parameter values in this example.

threads as in Figure 1d, the weave pattern can be seen and the vertical and horizontal thread densities can be determined. The spectral algorithm is rooted in the observation that the various layers of paint, including the ground that fills the canvas weave, additively contribute to the opacity term found in (1). Because the variations of x-ray intensity are relatively small and the tendency of x-ray film exposure to compensate for the exponential, *linear* processing algorithms are most appropriate for extracting thread counts.

## 2. SPECTRAL THEORY OF CANVAS WEAVE PATTERNS

A completely automatic spectral algorithm<sup>7</sup> takes advantage of the two-dimensional regularity of the canvas weave. A weave pattern is produced by the interleaved pattern of horizontal and vertical threads. A mathematical description of the x-ray of a paint-filled, ideal canvas-weave surface is difficult to determine, to say the least. A more phenomenological model is shown in Figure 2a. Here, the vertical and horizontal threads are shown as bars, each thread having its own thickness and weave density, that mimics the appearance of woven threads. The black rectangles are intended to represent unit-height rectangles and the white background represents zero. Thus, the black rectangles represent the top surface of the horizontal and vertical threads. The horizontal and vertical thread separations are  $D_h$  and  $D_v$ , respectively. Each horizontal and vertical thread's thickness and weave are captured by the widths and heights of the bars. For example, the horizontal threads have a thickness  $H_h$  and a width of  $W_h$ . The thicknesses and widths must satisfy  $D_v \geq \frac{W_h + W_v}{2}$  and  $D_h \geq \frac{H_h + H_v}{2}$ . To develop a mathematical expression for this pattern, define  $b_h(x, y)$  to be a bar corresponding to a horizontal thread.

$$b_h(x, y) = \begin{cases} 1 & |x| < \frac{W_h}{2}, |y| < \frac{H_h}{2} \\ 0 & \text{otherwise} \end{cases}$$

A similar expression applies to the vertical threads but parameterized by  $W_v$  and  $H_v$ . The entire weave pattern can be captured as a convolution of the basic thread shapes with a field of impulses that puts them at the proper locations.

$$c(x, y) = \left[ b_v(x, y) \otimes \sum_n \delta(x - 2nD_v) + b_h(x, y) \otimes \sum_n \delta(x - (2n + 1)D_v) \right] \otimes \sum_m \delta(y - 2mD_h) \\ + \left[ b_v(x, y) \otimes \sum_n \delta(x - (2n + 1)D_v) + b_h(x, y) \otimes \sum_n \delta(x - 2nD_v) \right] \otimes \sum_m \delta(y - (2m + 1)D_h) \quad (2)$$

By considering each part of this complicated expression, the model and Figure 2a can be reconciled. To express the top row of Figure 2a, the first line in square brackets uses convolutions to space the vertical-thread bars  $b_v(x, y)$   $2D_v$  apart

and the horizontal-thread bars  $b_h(x, y)$  by the same amount but shifted to the right by the vertical thread separation ( $D_v$ ). Continuing the first line, the convolution of this expression with impulses spaced by twice the horizontal thread separation  $2D_h$  creates the pattern of every other row. The expression in brackets on the second line shifts the first line's bracketed expression by the vertical thread separation and the outer convolution repeats it, interleaving it with the first line's pattern.

The Fourier transform of this expression can be found using basic transform properties: the transform of the sums of impulses become sums of impulses located at the separation harmonics and the interleaving shifts become phase terms. Gathering the expression for the spectrum into terms corresponding to the horizontal and vertical bars,

$$\begin{aligned} C(f_x, f_y) = & B_v(f_x, f_y) \cdot \left[ \sum_{m,n} \delta\left(f_x - \frac{n}{2D_v}\right) \delta\left(f_y - \frac{m}{2D_h}\right) \right. \\ & \left. + e^{-j2\pi f_x D_v} e^{-j2\pi f_y D_h} \sum_{m,n} \delta\left(f_x - \frac{n}{2D_v}\right) \delta\left(f_y - \frac{m}{2D_h}\right) \right] \\ & + B_h(f_x, f_y) \cdot \left[ e^{-j2\pi f_x D_v} \sum_{m,n} \delta\left(f_x - \frac{n}{2D_v}\right) \delta\left(f_y - \frac{m}{2D_h}\right) \right. \\ & \left. + e^{-j2\pi f_y D_h} \sum_{m,n} \delta\left(f_x - \frac{n}{2D_v}\right) \delta\left(f_y - \frac{m}{2D_h}\right) \right] \end{aligned}$$

The spectrum contains impulses located on a rectangular grid with centers at  $\left(\frac{n}{2D_v}, \frac{m}{2D_h}\right)$ , in other words at the half-harmonics of the basic thread counts (frequencies). Consequently, we need only evaluate the spectrum at these frequencies.

$$\begin{aligned} C\left(\frac{n}{2D_v}, \frac{m}{2D_h}\right) &= B_v\left(\frac{n}{2D_v}, \frac{m}{2D_h}\right) \left[1 + e^{-j\pi(n+m)}\right] + B_h\left(\frac{n}{2D_v}, \frac{m}{2D_h}\right) \left[e^{-j\pi n} + e^{-j\pi m}\right] \\ &= B_v\left(\frac{n}{2D_v}, \frac{m}{2D_h}\right) \left[1 + (-1)^{n+m}\right] + B_h\left(\frac{n}{2D_v}, \frac{m}{2D_h}\right) \left[(-1)^n + (-1)^m\right] \end{aligned} \quad (3)$$

The expressions for the Fourier transforms of the bars are

$$\begin{aligned} B_h\left(\frac{n}{2D_v}, \frac{m}{2D_h}\right) &= W_h H_h \operatorname{sinc}\left(\pi n \frac{W_h}{2D_v}\right) \operatorname{sinc}\left(\pi m \frac{H_h}{2D_h}\right) \\ B_v\left(\frac{n}{2D_v}, \frac{m}{2D_h}\right) &= W_v H_v \operatorname{sinc}\left(\pi n \frac{W_v}{2D_v}\right) \operatorname{sinc}\left(\pi m \frac{H_v}{2D_h}\right) \end{aligned} \quad (4)$$

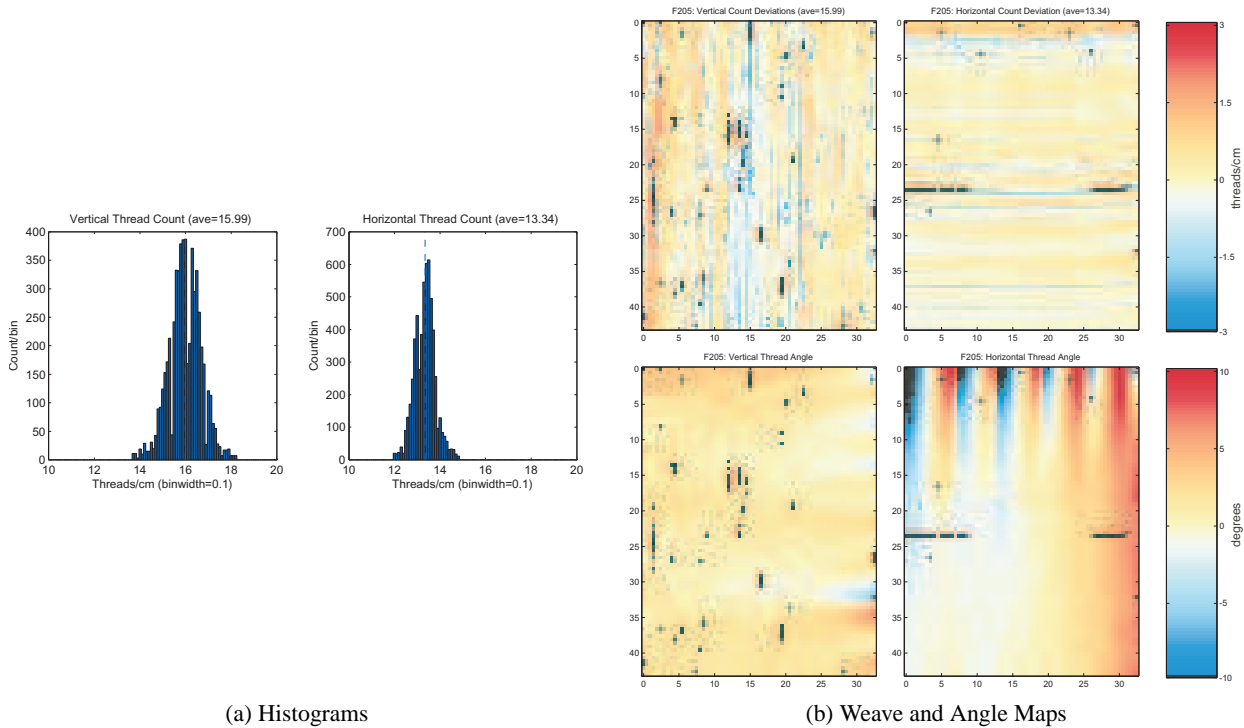
where  $\operatorname{sinc}(x) = \frac{\sin x}{x}$ .

To interpret the result in (3), note that when the sum of the indices  $n, m$  is odd, the spectrum is zero. Figure 2b shows the locations in the spectrum that can be non-zero. The spectra of the bars given by the previous expressions provide the spectral values at these frequencies. In general, the larger the frequency indices, the smaller these spectral values will be. The largest value is, of course, the origin. This peak provides no information about the weave pattern since its location does not depend on the canvas weave. Furthermore, it must be removed to produce accurate spectral estimates.\*

Note that the horizontal and/or vertical threads may not run in a precise straight line and that they are not usually parallel to the axes. These effects complicate traditional thread counting algorithms based on direct space-domain measurement, but have a ready frequency-domain interpretation. Slight thread curvature will create a slight widening of the spectral peak, but not its location. Weave rotations amount to a rotation of the ideal spectrum. The weave pattern can also be locally distorted due to attaching the canvas to a stretcher or priming frame at discrete points with tacks before applying the ground. Once the canvas dries from application of the ground, these weave pattern distortions remain, resulting in what is known as *cupping*. Such distortions amount to local deviations of the threads from their nominal directions, which results in a rotation of the spectral peaks for those threads. In either case, we cannot expect weave-pattern spectral peaks to lie on the frequency axes. These considerations led us to search for thread-count-related spectral peaks in wedge-shaped regions centered on the frequency axes (Figure 1e).

---

\*The current spectral thread counting algorithm highpass-filters the image before calculating spectra for just this reason.



(a) Histograms (b) Weave and Angle Maps

Figure 3: Thread counts in threads/cm and thread angles in degrees for the van Gogh painting F205 shown in Figure 1. The left side shows the unnormalized histograms of the measured horizontal and vertical thread counts. The center column shows a heat map of how the thread count measurements deviated from their respective averages: 13.33 threads/cm horizontally and 16.01 threads/cm vertically. Each square corresponds to a spectrum sampled every 1/2 cm across the surface in both  $x$  and  $y$ . Black pixels indicate where the algorithm made no thread-count estimates. The thread angles are also measured from the spectra and are shown in the right column. Manufacturer cusping induces the “rainbow” pattern found in the horizontal (warp) thread angles.

After highpass filtering, the spectral-based thread count algorithm computes two-dimensional Fourier transforms from raised-cosine-windowed, overlapping sections taken across the entire image, an approach we term “short-space” Fourier analysis. As indicated by our theory, peaks located near the vertical and horizontal axes are due to the periodic structure of the canvas weave. Figure 1e shows a typical spectrum of a section. Because of the possibility of weave pattern rotations, the radius of the selected spectral peak corresponds to the thread count. Peak locations are extracted from each spectrum, with a post-processing heuristic applied to resolve cases in which more than one spectral peak emerges because of weave inhomogeneities or “interference” from the artist’s work. We also measured the angle of the spectral peak and discovered that thread angle variations provide a clear visualization of cusping. Typical weave distributions, weave deviation (from average) and thread angle maps are shown in Figure 3. The histograms reveal that the vertical threads correspond to the warp direction on the original canvas roll (the criterion is a smaller spread of the thread count distribution). Typical of our investigations, the warp-direction weave maps show a fine, more consistent variability than do the weft-direction maps. The weave maps indeed show systematic variations in both the warp and weft directions, a kind of “fingerprint” for the canvas, not the painting, that can be compared with other paintings. The angle maps markedly indicate the presence of cusping of the warp threads along the painting’s top edge and nowhere else, reinforcing the conclusion that this cusping occurred during commercial priming and that the painting’s top edge corresponds to an edge of the canvas roll. To find other paintings that could have come from the same roll, we need an algorithm that finds matching spatial weave variations and locates the paintings’ relative positions in space.

### 3. WEAVE MAP MATCHING

Using the convention that the warp direction is vertical, paintings made from canvas cut to the left or right of an analyzed painting should share the same variation pattern in weft while one cut from above or below should share the same warp

variations. Because of the striping in both the vertical and horizontal weave maps, we averaged the vertical and horizontal counts along thread direction to create thread count *profiles* for the vertical and horizontal directions. Thus, for the horizontal thread counts, weave map values in each row were averaged; for the vertical thread counts, columns were averaged. For painting locations where no count was made, no value contributed to the average. We demanded a minimum number of counts contribute to the average; otherwise, no value was provided for the profile at that point. With these one-dimensional summaries of thread density variations, searching for matching x-rays having matching variations can be accomplished with a cross-correlation technique. Because painting orientation cannot be presumed to agree with canvas orientation, taking the various possibilities into account means correlating combinations of profiles and their reversed versions: if  $v_i$ ,  $h_i$  represent the vertical and horizontal profiles for the  $i^{\text{th}}$  paintings respectively and  $\text{rev}(v_i)$  the reversed version of  $v_i$ , the following eight pairs of correlations must be considered so as to take into account the various rotations a canvas support can undergo once it is cut from a roll and attached to a stretcher for painting:  $v_i \leftrightarrow v_j$ ,  $h_i \leftrightarrow h_j$ ,  $v_i \leftrightarrow h_j$ ,  $h_i \leftrightarrow v_j$ ,  $v_i \leftrightarrow \text{rev}(v_j)$ ,  $h_i \leftrightarrow \text{rev}(h_j)$ ,  $v_i \leftrightarrow \text{rev}(h_j)$ ,  $h_i \leftrightarrow \text{rev}(v_j)$ . We took the maximum of these correlations as the potential weave match between two paintings, with a weave match declared if the correlation was sufficiently large.

Several issues arise when using the usual cross-correlation function normalized to produce a correlation coefficient. First of all, the profiles amount to small deviations added to a large constant. For example, the warp variations of F205 shown in Figure 3 is  $\pm 1$  thread/cm about an average of 13.3 threads/cm. Because of the non-zero offset, the raw cross-correlation function will be insensitive to the much smaller thread density variation. Secondly, if each profile's average is subtracted to remove the constant term, the normalization that is part of computing the correlation coefficient will not take into account the scale of the deviations. Because of these issues, a new cross-correlation method was developed. The correlation coefficient is rooted in the Cauchy-Schwarz inequality:  $|\langle x, y \rangle| \leq \|x\| \cdot \|y\|$ . The problem is that equality, equivalent to maximal correlation, occurs when  $x \propto y$ . We demand maximal correlation when the two quantities are equal, not just proportional. Simple manipulations lead to what might be called the maximal *linear* correlation coefficient.<sup>†</sup>

$$|\langle x, y \rangle| \leq \|x\| \cdot \|y\| \leq \max\{\|x\|^2, \|y\|^2\}$$

Now, dividing the inner product by the maximum squared norm yields a value of one only when  $x = y$ . Note that if a constant is subtracted from each the same result applies:  $|\langle x - m, y - m \rangle| \leq \max\{\|x - m\|^2, \|y - m\|^2\}$ . Removing the average thread count in this way leads to a similarity measure that focuses on the same waveform and amplitude of weave deviations. We take  $m$  to be the average of the two profile's average. Thus, if the two profile's averages differ, the maximal linear correlation coefficient will be reduced. The resulting maximal cross-correlation function is

$$r_{i,j}(\ell) = \frac{\sum_m [w_i(m) - \bar{w}] \cdot [w_j(m - \ell) - \bar{w}]}{\max\{\sum_k [w_i(k) - \bar{w}]^2, \sum_l [w_j(l - \ell) - \bar{w}]^2\}},$$

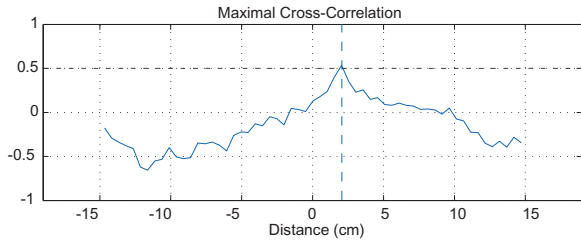
where  $w_i$  represents  $v_i$  or  $h_i$  as appropriate. We further demanded that at least 10 cm of canvas overlap in the cross-correlation calculations.

Figure 4 shows the maximal linear cross-correlations between two pairs of paintings that illustrate warp and weft-direction weave matches. F205's vertical threads correspond to weft threads and its weave pattern matches that of F260 (again vertical threads). Note that the cross-correlation peak is broad, which lessens the precision of the alignment. Such broad cross-correlation peaks typify weft-direction weave matches. In depicting and describing weave matches, warp threads run vertically and weft threads horizontally. Thus, this weft match means that the canvas supports for these paintings were cut from the same canvas roll, side-by-side. The weave maps for the paintings F597 and F748 match in warp, the more consistent direction. The maximal linear cross-correlation value for this case was 0.76; the peak is broader than other warp-direction matches we have found. In general, we have found that cross-correlation functions for warp-direction matches are far narrower than weft-direction matches and produce larger correlation values (exceeding 0.95 in some cases). This warp-direction match implies that the supports for the paintings were cut from the same canvas bolt one above the other.

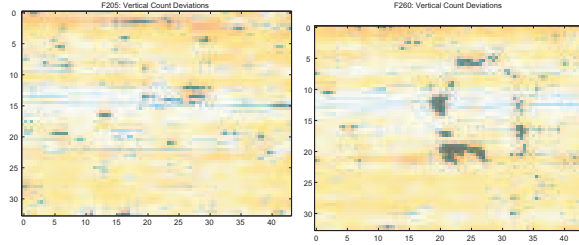
We need to understand the underlying reason for these cross-correlation function differences, which leads to needing a criterion for thresholding the cross-correlation function that incorporates the differing characteristics of warp and weft

---

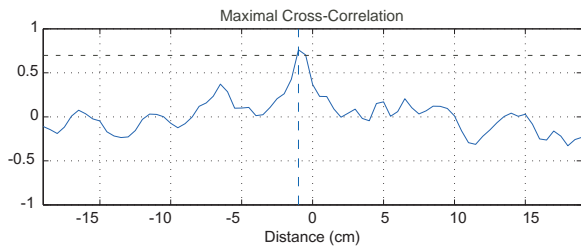
<sup>†</sup>The maximal correlation coefficient between two random variables  $X$  and  $Y$  is defined as the maximal value of  $\text{cov}\{\phi(X), \eta(Y)\}$  with respect to all possible functions  $\phi(\cdot), \eta(\cdot)$ .



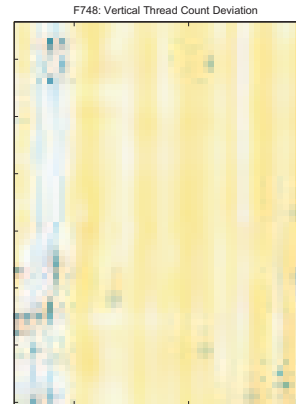
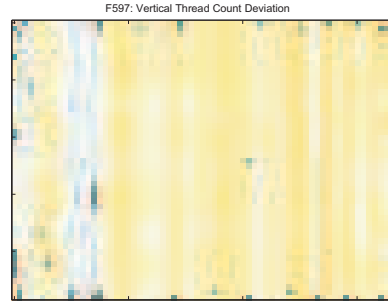
(a) Cross-Correlation: F205 and F260



(b) Weave Maps: F205 and F260



(c) Cross-correlation: F597 and F748



(d) Weave Maps: F597 and F748

Figure 4: Panel (a) shows the maximal cross-correlation function between the vertical (weft) weave patterns of F205 and F260. The convention is that the weave maps are rotated to mimic their position on a canvas roll: horizontal is the weft direction and vertical is warp. Panel (b) shows both painting's weave maps, with the weave maps aligned according to the correlation function peak. Panels (c) and (d) shows the same quantities for van Gogh's paintings F597 and F748, this time illustrating a warp weave pattern alignment. A clear correlation peak is evident for the vertical (warp) threads once F748 was rotated  $180^\circ$ . The threshold for peak correlation for warp matches is indicated by the horizontal dashed line.

weave patterns. We model the profiles that summarize two weave patterns as statistically independent, identically distributed random processes  $w_i(n)$ ,  $w_j(n)$ , which makes the expected value of the empirical cross-correlation is zero. What is of interest is the probability that this cross-correlation exceeds a threshold despite the two profiles being unrelated. We shall assume the quantity  $\hat{R} = \sum_n w_i(n)w_j(n)$  is approximately Gaussian, which means we only need to evaluate its variance to estimate the probability that the cross-correlation exceeds a threshold.

$$\mathbb{E}[\hat{R}^2] = \frac{1}{N^2 R^2(0)} \left( NR^2(0) + 2 \sum_{\ell=1}^{N-1} (N-\ell) R_1(\ell) R_2(\ell) \right)$$

Here,  $N$  denotes the number of values in the cross-correlation function estimate and is equivalent to the length of canvas over which two weave maps are compared. The most interesting case has equal correlation functions: the two profiles have the same statistical structure but are statistically independent of each other. After simplification that incorporates this

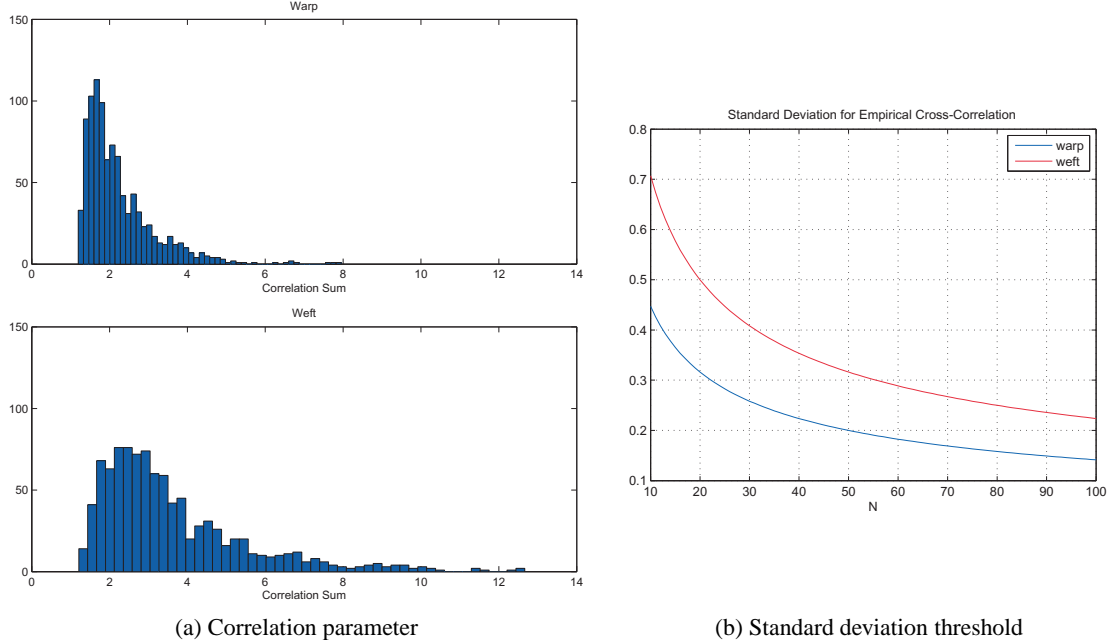


Figure 5: Panel (a) shows the bracketed term in (5) for the warp and weft thread weave patterns drawn from paintings by van Gogh in our database. Panel (b) plots the square root of (5) using average values for the bracketed term. The lower curve is  $\sqrt{2/N}$ , the upper  $\sqrt{5/N}$ , where  $N$  is the number of values used in the cross-correlation.

assumption, we have

$$\mathbb{E}[\widehat{R}^2] = \frac{1}{N} \left[ 1 + 2 \sum_{\ell=1}^{N-1} \left( 1 - \frac{\ell}{N} \right) \rho^2(\ell) \right] \quad (5)$$

where  $\rho(\ell)$  is the correlation-coefficient function.

To estimate the variance, we computed the term in brackets for the every x-ray in the van Gogh database. In this database, each weave pattern was marked as representing the warp or weft direction. The result for the two directions is shown in Figure 5a. Clearly, the weft thread pattern tends to yield larger correlation variances than the warp, the reason being the lower-frequency nature of weft-thread count variations in the warp direction. Because of histogram spread, no typical value portrays the behavior. Figure 5b shows square-root of (5), the standard deviation, for two values of the bracketed term. With this plot, thresholds for declaring a significant cross-correlation can be established, as well as determining the smallest overlap that can yield acceptable results. With a Gaussian model, an empirical cross-correlation exceeding two standard deviations is very low:  $\Pr[\widehat{R} > 2\sigma] = 0.023$ . This rule-of-thumb can be used to determine a threshold. For example, at a 0.5 cm evaluation interval for weave maps, a 10 cm canvas overlap has  $N = 20$  values in the cross-correlation function estimate. A two-standard-deviation threshold would thus be about 0.6 for the smaller value of the bracketed term but 1.0 for the larger, an unreasonable value. To achieve the same reliability for what might be a weft match having the larger value, at least 50 values must be used in the estimate (25 cm of overlap is required). This analysis indicates why weft matches tend to be more difficult to discern from individual x-rays (in that many false-positives occur).

#### 4. RESULTS

To date, x-rays made from a total of 292 paintings by van Gogh<sup>‡</sup> have been analyzed for thread-count and angle maps and processed for any viable weave matches. To date, thirty cliques of paintings exceed our threshold for declaring a weave match in either warp or weft. We are currently examining these cliques in detail, but one clique of forty-four paintings stands out. The weave matches also include the thread angles: paintings placed along the edges because of the wave match all indicate primary cusping, confirming their putative placement along a canvas roll edge. All of these were painted on pieces of “ordinary” quality canvas cut from commercially primed rolls, which van Gogh is known to have customarily

<sup>‡</sup>His output is well over 800 paintings. Consequently, less than one-third of van Gogh’s painting output has been examined.

ordered from the Paris company Tasset et L'Hôte in the late French period of his production. Painting positions enforced by warp matches span the width of a commercial canvas roll (2m) and extend over a minimum length of 12m (rolls had a maximum length of 10m). If indeed these paintings were made on sections cut from the same roll of canvas, the datings suggest that the same canvas roll was used over a period of at least eighteen months and two residence changes. We believe this an unlikely possibility. Instead, we conclude that our method identifies canvas rolls cut from the same *bolt* of cloth supplied to the commercial priming company.<sup>8</sup> A chemical analysis of the ground would contribute additional information so that this clique could be objectively separated into sub-cliques based on sharing several measurements.

## 5. CONCLUSIONS

Signal processing has shown to play an important role in determining authenticity, as well as helping to date works and provide a better understanding of the sequence of artists' production. Whereas the signal processing tools described in<sup>1</sup> consider colors and brushstrokes evident at the paint surface, the algorithms outlined here help to fingerprint the different types of canvas picture support used. Automatic techniques based on two-dimensional spectral analysis weave estimation and correlation techniques have provided far more information about the weave than has been possible to date. Together, these different signal processing measurements provide valuable new insights into the artist's technical and creative processes, complementing traditional types of information gained by chemical analysis of painting materials and study of historical sources.

As the size of the database increases to include artists' works spanning four centuries, we are learning the variety of weave patterns used in manufacturing artist canvas. These patterns have different spectra,<sup>9</sup> most of which are dominated by horizontal and vertical peaks. We have derived the spectra these weave patterns yield and have developed accordingly spectral algorithms that can cope with all that have been seen to date. In this way, we hope to move toward our goal of a truly automatic thread counting algorithm that provides detailed information for weave matching algorithms.

## ACKNOWLEDGMENTS

The authors thank the many museums that contributed to the database of scanned x-ray images of van Gogh's paintings.

## REFERENCES

- [1] Johnson, Jr., C., Hendriks, E., Berezhnoy, I., Brevdo, E., Hughes, S., Daubechies, I., Li, J., Postma, E., and Wang, J., "Image processing for artist identification," *Signal Processing Magazine* **25**, 37–48 (July 2008).
- [2] Lister, K., Peres, C., and Fiedler, I., "Appendix: Tracing an interaction: Supporting evidence, experimental grounds," in [*Van Gogh and Gauguin: The Studios of the South*], Druick, D. and Zegers, P., eds., 354–369, Thames & Hudson (2001).
- [3] van de Wetering, E., [*Rembrandt: The Painter at Work*], Amsterdam University Press, Amsterdam (1997).
- [4] Kirsh, A. and Levenson, R., [*Seeing through Paintings: Physical Examination in Art Historical Studies*], Yale University Press (2000).
- [5] Klein, A., Johnson, D., Sethares, W., Lee, H., Johnson, Jr., C., and Hendricks, E., "Algorithms for old master painting canvas thread counting from x-rays," in [*Asilomar Conference on Signals, Systems and Computers*], (2008).
- [6] de la Faille, J.-B., [*The Works of Vincent van Gogh: His Paintings and Drawings*], Meulenhoff, Amsterdam (1970).
- [7] Johnson, D., Johnson, Jr., C., Klein, A., Sethares, W., Lee, H., and Hendriks, E., "A thread counting algorithm for art forensics," in [*DSP Workshop*], (2009).
- [8] Henriks, E., Johnson, D., and C.R Johnson, J., "Interpreting canvas weave matches," *Art Matters* (2010). Submitted.
- [9] Escofet, J., Millán, M., and Ralló, M., "Modeling of woven fabric structures based on Fourier image analysis," *Applied Optics* **40**, 6170–6176 (2001).